Interictal Spike Classification in Pharmacoresistant Epilepsy using Combined EEG and MEG

1st Glykeria Sdoukopoulou
School of Electrical and Computer Engineering
Technical University of Crete
Kounoupidiana, Chania, Crete, Greece
gsdoukopoulou@isc.tuc.gr

2nd Marios Antonakakis
School of Electrical and Computer Engineering
Technical University of Crete
Kounoupidiana, Chania, Crete, Greece
mantonakakis@isc.tuc.gr

3rd Gabriel Möddel
Department of Neurology
Münster University Clinic (UKM)
Albert-Schweitzer-Campus, 48149 Münster, Germany
Gabriel.Moeddel@ukmuenster.de

4th Carsten H. Wolters
Institute of Biomagnetism and Biosignalanalysis
University of Münster
Malmedyweg 15, 48149 Münster, Germany
carsten.wolters@uni-muenster.de

5th Michalis Zervakis
School of Electrical and Computer Engineering
Technical University of Crete
Kounoupidiana, Chania, Crete, Greece
michalis@display.tuc.gr

2021 IEEE 21st International Conference on Bioinformatics and Bioengineering (BIBE) | 978-1-6654-4261-9/21/$31.00 ©2021 IEEE | DOI: 10.1109/BIBE52308.2021.9635501

***Abstract*—Epilepsy is one of the most common brain disorders worldwide. The basic principle in epilepsy is to resect the epileptogenic zone (EZ) when the medicaments are inadequate to suppress epileptic seizures. Epilepsy is accompanied by interictal spikes, a surrogate marker serving as an identifier of seizures. The automatic temporal detection of these spikes is of major importance due to the demanding time consumption of the manual annotation. Electro- and magneto- encephalography (EEG and MEG) are the most usual measurement modalities for the recording of brain activity. EEG and MEG are ideal modalities for the non-invasive monitoring of drug-resistant epilepsy. Many approaches have been proposed for the temporal detection of interictal spikes. However, only single measurement modality (EEG or MEG) has been used up to now, neglecting their complementary content. In this study, we develop a multi-feature and iterative classification scheme with input from either single modality (EEG or MEG) or combined EEG/MEG (EMEG). The inputs include statistical (kurtosis and Renyi Entropy) and spectral (Energy) features as well as the functional connectivity metrics, global and local efficiency from imaginary phase lag index networks. The classification performance for all modalities ranges from 89% to 92.8%, with the maximum performance being observed for EMEG. Overall, the complementarity of EEG and MEG on the detection of interictal spikes is promising, opening new considerations on the development of automatic epileptic spike detection approaches.**

***Index Terms*—epilepsy, automatic spike detection, SVM, EEG, MEG, classification**

I. Introduction

Epilepsy accounts for one of the most common brain disorder affecting more than 50 million people worldwide and almost two million people in Europe [1]. A percent of those cases remain resistant to any known combination of antiepileptic drugs, making surgery, the most promising alternative treatment [2], [3]. The main principle of epilepsy surgery is to resect the epileptogenic zone, the cortical area in which epileptic seizures can appear [4]. In order to proceed with surgery, the epileptogenic zone (EZ) has to be localized with sufficient accuracy. To adequately indicate the EZ, interictal spikes are widely used as a well-established biomarker [5].

Invasive electrophysiological measurements of those spikes with the use of intra-cranial Electroencephalography (iEEG) is the most common method to localize precisely the EZ. However, iEEG is an invasive method that needs assistance to localize or indicate successfully EZ [4]. Electroencephalography (EEG) and magnetoencephalography (MEG) are non-invasive types of brain activity measurement that are used for the guidance of iEEG or even indication of EZ [4]. Due to their high temporal resolution and their relatively easy and comfortable use, EEG and MEG have been extensively used for monitoring brain activity and recording interictal spikes. Due to their complementary nature [6], [7], [8], [9], their simultaneous acquisition can detect interictal spikes located in a different side of a specific cortical patch [10], [11], [12]. At a report series of 297 consecutive patients, Ebersole and Wagner [12], showed that an 8% of all spikes were detected in MEG alone, whereas 36% in EEG alone.

In many cases, a set of interictal spikes is annotated manually by board certified epileptologists. However, such a procedure is quite demanding and laborious, making the need of automatic detection procedures the only alternative. General classification approaches, using mimetic, spikes templates or

spike-specific characteristics (i.e. peak) [13], [14] have been exploited. Recently, machine and deep learning approaches gained considerable ground. Weber [15] developed an artificial neural network detector with sensitivity equal to 73%. Gabor and Seyal [16] combined time domain features with an error-back-propagation feed-forward neural network classifier with a sensitivity of 94.2% [14]. One of the few Spike detectors on MEG data implemented by Khalid [17] used Common Spatial Filters (CSPs) for feature extraction and Linear Discriminant Analysis (LDA) for classification with sensitivity and specificity equal to 91.03% and 94.21%, respectively. Inan and Kuntalp [18] implemented a neural pre-classifier and a Fuzzy C-Means (FCM) with sensitivity and specificity equal to 93.3% and 74.1%, respectively. Feuchet [19] combined instantaneous power computed by Hilbert Transform with a Multilayer Perceptron (MLP) reaching an average sensitivity and specificity of 88.1% and 89.3%, respectively. Tjepkema-Cloostermans [20] implemented a neural network based spike detection algorithm, tested only on EEG data with AUC, sensitivity and specificity equal to 94%, 47.4% and 98.0%, accordingly. Similarly, Lourenço [21] applied a VGG CNN on EEG data. To increase scheme's performance, the data were augmented by applying temporal shifting and using different EEG montages. Sensitivity increased from 63% to 96% at 99% specificity. However, none of these studies utilize the complementary content of EEG and MEG measurement modalities [6]–[8], [22].

In the present study, we used machine learning techniques to automatically detect interictal spikes not only on the extracted signal features of EEG, and MEG data but also on the combination of them, EMEG data. In our procedure, we propose the estimation of multiple features based on the statistical and spectral analysis of the signals as well as network connectivity metrics based on the estimation of the imaginary part of coherency alleviating volume conduction effects [23]. After feature extraction, we then assess the performance of two proven classification algorithms with the use of iterative stratified cross-validation schemes.

II. Patient and methods

A. Ethics Statement

All the procedures took place after the written consent of the patient and have been approved by the local ethics committee, as well as by the ethics committee of the University of Erlangen (Ref No 4453 B).

B. Patient's Electrophysiological Data

In this study, we analyzed the electrophysiological data (EEG and MEG) of a twenty-year old female patient. The patient suffered from pharmacorestistant epilepsy since the age of 14 without affecting her intellectual abilities and focal neurological deficit. The seizure semiology was described as distributed thinking and inability to speak or follow a conversation, without any motor symptoms and without impairment of awareness. Initially, a medical treatment was not fully successful (indication of a drug-resistant case), leading to a presurgical evaluation for possible resective epilepsy surgery.

The data were acquired with an EEG and MEG recording system while the patient was in supine position. Specifically, eighty AgCl sintered ring electrodes (EASYCAP GmbH, Herrsching, Germany [1], 74 channel EEG plus additional 7 channels to detect eye movements and heart artifacts) were conducted for EEG and a whole-head MEG system with 275 axial gradiometers and 29 reference coils (OMEGA2005, CTF, VSM MedTech Ltd., Canada [2]) for MEG. Six runs were acquired in total to annotate possible interictal spikes on the resting state brain activity. The runs were 8 min long with a sampling rate at 2400Hz.

C. Preprocessing

The first step of EEG/MEG processing included filtering and reduction of the non-cerebral activity. After the baseline correction of the raw EEG/MEG recordings, a notch filter was applied to reduce the power line noise component at 50 Hz and its harmonics. Then, using a digital band-pass filter, the recordings were filtered between 1 and 100 Hz. Measurements were visually inspected for the exclusion of "bad" channels, EEG and MEG channels that contain highly noise activity and cannot be further analyzed. The detected "bad" channels TP9, P6, O9, Iz, P10, MLT44, MLT47, MLT55, and MLT56 were excluded from the analysis. The ocular and cardiac artifacts were detected based on a matching of the measurements with the recorded EEG ocular and cardiac activity followed by visual inspection of the candidate non-cerebral activity in each EEG/MEG modality.

The interictal spikes were manually identified and marked by two experienced epileptologists on the artifact-free EEG and MEG continuous data. The final number of spikes was 1050, after the annotation of the two evaluators. Each spike peak was aligned around the zero time point and a trial with time duration 400 ms (200 ms before and after the spike peak) was defined. The electrode F3 was used as reference since it presented the highest negativity compared to the rest channels. Non-Spike trials with time duration of 400 ms were randomly extracted from the EEG/MEG data independently, with no overlapping with the Spike trials. The number of extracted Non-Spike trials was 1050.

The final step of the data preprocessing was the combination of EEG and MEG data. The EEG/MEG artifact-free trials were vertically concatenated and then the whitening transformation was applied, according to the noise level of each channel. As noise, we considered the time window between -400 ms to -200 ms before the spike peak. The whitening approach was followed to obtain unitless EMEG trials for further analysis [22].

D. Feature extraction

As explained in Section III. Results, a variety of features was extracted from each modality (EEG, MEG and EMEG)

[1]https://www.easycap.de
[2]https://www.ctf.com

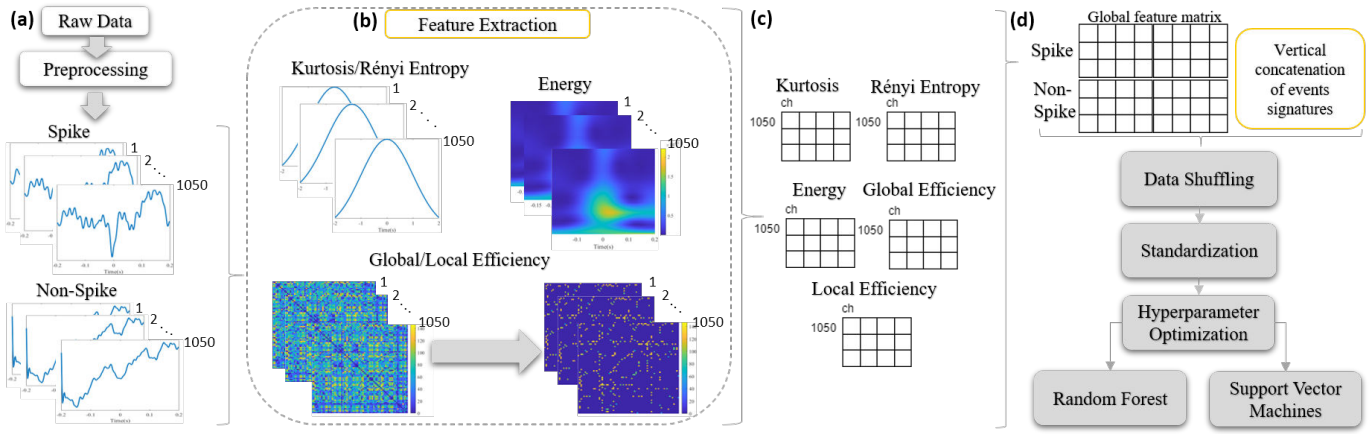

Fig. 1. Overview of the proposed Spike detection pipeline. Spike and Non-spike trials were categorized as two different event types. **(a)** After the preprocessing of the raw data, 1050 Spike and 1050 Non-Spike trials were extracted from each modality, EEG and MEG. For EMEG, the EEG and MEG Spike and Non-Spike trials were vertically concatenated and whitened. The feature extraction approach was applied independently for EEG, MEG and EMEG. **(b)** Features were extracted for each trial, constructing a matrix with dimensions $1050xch$, where 1050 is the number of events (Spike or Non-Spike) and ch denotes the number of channels. **(c)** After all features had been extracted from each event type, they were vertically concatenated creating a global feature matrix. **(d)** The global feature matrix was fed into the classification scheme.

comprising a global matrix which was fed into the classification scheme.

1) Time domain features: The extracted time domain features were kurtosis (forth standardized moment) and Rényi entropy. Kurtosis as a measure of extreme values at the tails of a distribution gives a good insight about the differences between a Spike and a Non-Spike. A spike is characterized by a specific morphological pattern with a peak, while a Non-Spike appears as a random signal state [24], [25]. On the same basis, Rényi entropy as a measurement can identify the repeated pattern of a Spike and the randomness of a Non-Spike [26], yielding higher values for the second case. To our best of knowledge, this is the first time, that Rényi entropy is examined for the identification of interictal spikes.

2) Frequency domain features: The spectral content of the EEG/MEG data contains useful information about the Spike and Non-Spike trials (Fig. 2). Interictal spikes, except their characteristic pattern on time domain, show a unique frequency fingerprint as a restricted island [27]. This frequency signature denotes an energy accumulation at specific frequency-time ranges, unseen at the random Non-Spike events. Consequently, the total energy spectrum was a spectral feature calculated as the square value of the absolute Discrete Fourier Transform (DFT) coefficients [25].

3) Network metrics: In this study, we also estimated the pairwise relation between pairs of channels by means of imaginary part of phase lag index (iPLV). In this manner, we intended to embed in our classification scheme, the functional interactions among channels expressed as connectivity graphs. The bivariate metric iPLV was selected due to its sensitivity to non-zero-phase lags [28]. Given a pair of two phase signals, $\phi_x(t)$ and $\phi_y(t)$, derived from the application of the Hilbert transformation to the original signals $x(t)$ and $y(t)$, the iPLV is described as follows:

$$iPLV_{xy} = \left|im(\sum_i e^{i(\phi_x(t)-\phi_y(t))/N})\right|,$$

where N is the number of samples and and $|.|$ denotes the absolute value operator [29]. To enhance the most significant connections on the connectivity graphs we applied a topological filtering based on graph theory principles and data-driven thresholding.

To study the structure of the neural system we were interested in, topological filtering based on graph analysis was used [30], [31]. To quantify the functional relation in a row, we used the network metrics Global and Local efficiency for each estimated connectivity graph. Global efficiency was defined as the average inverse shortest path length in the network [29], [32]. Local efficiency, a segregation measure, was computed as the global efficiency on node's i neighborhood [29], [32].

E. Classification scheme

The proposed classification scheme comprises of a feature shuffling and scaling step, tuning of the classifiers' hyperparameters and final classification using two different classifiers [33]. Standardization was used as a feature scaling method to restrict feature value range. As a subset of a classifier's hyperparameters can significantly affect the cross-validation score, an optimization of the hyperparametrs value was implemented. Optimal values were obtained by an exhaustive search on a user-defined parameter grid. Hyperparameters optimization was implemented for the examined classifiers, Random Forest (RF) [33] and Support Vector Machines (SVM) [33], independently.

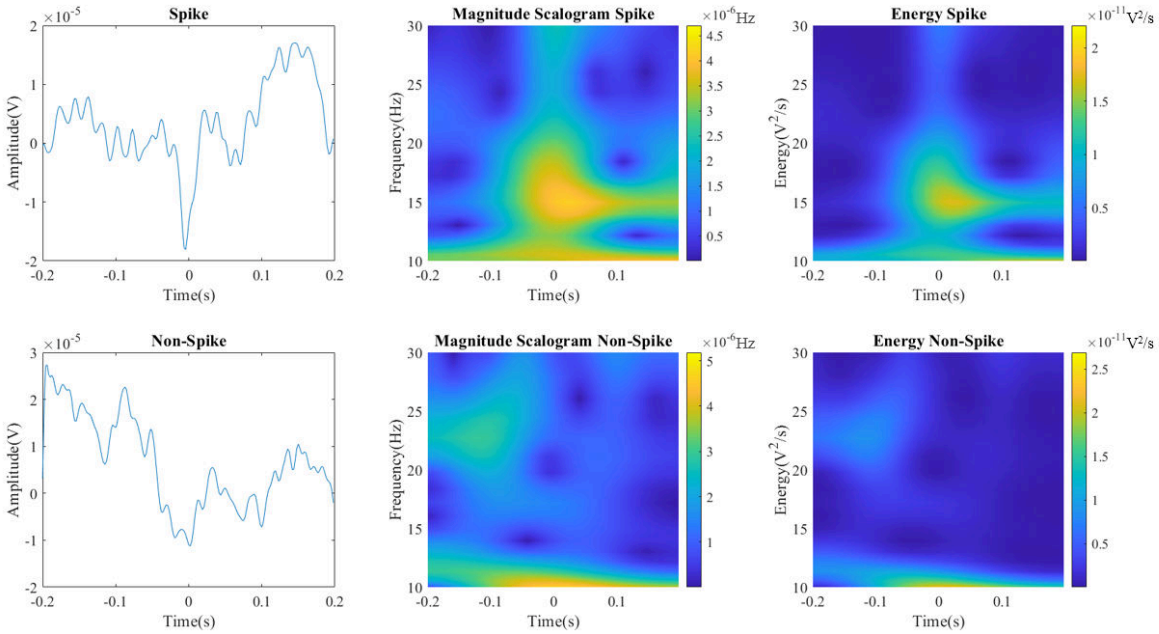

Fig. 2. A characteristic example of a Spike (upper row) and Non-Spike (lower row) event at time, time-frequency domain and their corresponding energy. At the left column, the characteristic Spike peak at the time is illustrated. At the middle column, the corresponding events are represented at the time-frequency domain as magnitude scalograms. At the Spike's scalogram (middle row, upper figure) its frequency signature stands out from the background as a resctricted activity. As expected the Spike's energy is concentrated at the frequency and time range denoted by the magnitude scalogram plot.

Repeated Stratified k-fold cross-validation was used to validate the classifiers' performance. Specifically, the data were split into k consecutive folds, where each fold was used as test set and the remaining folds as training sets. Each fold contained equal sample percentages of both classes and each repetition of Stratified k-fold cross validation was differently randomized. To evaluate the classifiers performance the scoring parameters *Accuracy, Precision, Recalls* and *F1s* were calculated and defined as follows:

- $Accuracy = \frac{TP+TN}{TP+FP+FN+TN}$
- $Precision = \frac{TP}{TP+FP}$
- $Recall = \frac{TP}{TP+FN}$
- $F1s = 2\frac{Precision\dot{R}ecall}{Precision+Recall}$,

where TP stands for True Positive, FN for False Negative, TN for True Negative and FP for False Positive.

III. Results

As a binary classification problem, Spike detection requires a targeted feature extraction approach summing up to a signature feature matrix for the Spike and Non-Spike events. Our approach is tested on three different datasets, EEG, MEG and EMEG. As explained in Section I. Introduction, EMEG detects a wider spectrum of spike types, a paramount trait we aim to exploit applying the classification scheme on the unitless EMEG dataset.

TABLE I
Hyperparameter Optimization

Classifier	Modality	Hyperparameter	Optimal value
RF	EEG	bootstrap	False
		max_depth	20
		min_samples_leaf	4
		min_samples_split	2
		n_estimators	150
	MEG	bootstrap	False
		max_depth	50
		min_samples_leaf	2
		min_samples_split	6
		n_estimators	300
	EMEG	bootstrap	False
		max_depth	50
		min_samples_leaf	1
		min_samples_split	6
		n_estimators	150
SVM	EEG	C	100
		gamma	0.0001
		kernel	RBF
	MEG	C	10
		gamma	0.0001
		kernel	RBF
	EMEG	C	10
		gamma	0.0001
		kernel	RBF

The pipeline followed is illustrated at Fig. 1. Specifically, for each measurement modality, EEG, MEG and EMEG, features were extracted independently, creating three global feature

TABLE II
CLASSIFICATION RESULTS

Modality	Classifiers	Accuracy	Precision	Recalls	F1
EEG	Random Forest	89.3 ± 1.4	92.5	85.5	88.8
	SVM (RBF)	89.0 ± 1.4	92.3	85.2	88.6
MEG	Random Forest	87.5 ± 1.5	89.9	84.5	87.1
	SVM (RBF)	90.1 ± 1.2	93.2	86.5	89.7
EMEG	Random Forest	92.5 ± 1.2	94.2	90.5	92.3
	SVM (RBF)	92.8 ± 1.1	95.1	90.2	92.6

matrices. The proposed classification scheme was evaluated for each global feature matrix independently. All features were calculated independently for each event type (Spike and Non-Spike). Consequently, each feature is represented as a matrix with dimensions $1050xch$, where 1050 is the number of events and ch stands for the channels.

The connectivity matrices were calculated based on iPLV for each event. Therefore, the connections were filtered out so that the pattern with the most significant connections could emerge. The topological filtering we performed was based on graph theory principles and data-driven thresholding [29].

For the global feature matrix construction, the vectorized approach was used [33]. Specifically, we concatenated horizontally the individual feature matrices of each event type creating a Spike and Non-Spike signature to explain them sufficiently. The global feature matrix was the vertical concatenation of the Spike and Non-Spike signatures. At Fig. 2 an example of a Spike and Non-Spike event with the corresponding magnitude scalograms and energies are shown. The characteristic spike fingerprint is not visible only on time domain. The magnitude scalogram, as a time-frequency representation, illustrates the Spike's unique fingerprint. Therefore, a Spike contains an increased amount of energy, differentiating from a random signal trial.

After completing the feature extraction step, we proceeded with the evaluation of the classification scheme, which was fed with each global feature matrix. Firstly, the data were shuffled and standardized. To find the optimal hyperparameters for each classifier, we defined the parameters grid: *(1) RF: 'n_estimators'*: [25, 50, 100, 150, 300], *'max_depth'*: [20, 30, 50], *'min_samples_split'*: [2, 4, 6], *'min_samples_leaf'*: [1, 2, 4], *'bootstrap'*: [True, False], *(2) SVM: 'C'*: [0.001, 0.10, 0.1, 10, 25, 50, 100, 1000], *'gamma'*: [0.001, 0.0001], *'kernel'*: ['rbf', 'linear']. Table I displays the optimal values for each classifier and modality.

The cross validation was repeated 1000 times and the number of stratified folds was 5. The evaluation metrics were calculated as the mean value of the repetitions. For *Accuracy*, we also calculated the standard deviation. Table II shows the classification results for each studied case. For EEG and MEG data, both classifiers reached an *Accuracy* score close to 90% percent with a low standard deviation. SVM estimated better the MEG Spikes with a high *Accuracy* score of 90.1%, a low standard deviation of 1.2% and a trade-off between *Precision* and *Recall (F1)* equal to 89.7%.

Overall, the synergy of EEG and MEG, EMEG, significantly outperformed both single measurement modalities yielding an *Accuracy* score equal to 92.5% for RF and 92.8% for SVM. In both cases, the standard deviation was majorly small, proving the classification scheme robustness. The paramount metric *F1* with a score of 92.3% and 92.6% for RF and SVM, respectively, elaborates that a minor percentage of Spikes and Non-Spikes was miss-classified; an important observation as Spikes and Non-Spikes miss-classification can propagate serious errors on further analysis steps such as the EZ indication (Section I. Introduction).

IV. DISCUSSION

In this study, we developed an iterative classification scheme for the accurate detection of interictal spikes. Firstly, we estimated statistical, spectral and channel synchronization-based features, representing an essential content of the signal. The classification scheme was examined for each measurement modality (EEG, MEG and EMEG), separately. After the essential optimization of the hyperparameters, two classification algorithms were examined. Their performance within iterative stratified k-fold validation scheme led to higher than 85% for single modality while the combination of EEG and MEG led to higher and less deviant results ($> 90\%$). Such classification performances show a promising window for future studies about the accurate detection of interictal spikes with the utilization of the complementary information of EEG and MEG.

A binary classification scheme using Machine Learning approach is a two step process; *(1)* a targeted feature extraction, explaining adequately the data to be detected and *(2)* building a robust classification scheme. As showed in Section II-D Feature extraction, we shown Spike unique pattern and characteristics by means of the extracted features (Kurtosis, Rényi entropyi, Energy, Global and Local Efficiency). An indispensable part of improving classifiers performance is also the hyperparameters optimization. The exhaustive grid search yielded the combination of optimal values for a subset of classifiers hyperparameters. It is important to notice that the use of default hyperparameters might lead to less optimal results, making the exhaustive grid search essential.

In the present study, we employed EMEG for interictal spike detection, leading to high classification performances. Previous studies on automatic spike detection approach the problem with different methods. The majority of those studies implemented a thresholding-based classification technique based on statistical and morphological characteristics [14]. Artificial Intelligence methodologies gradually gain ground on the spike detection field [15], [16], [18], [19], [34]–[36]. In both cases the Spike detection schemes have been tested mainly on EEG data, with a few cases on MEG [14], [17], [37]. In this study we went one step further exploring the dynamics of the combined EEG and MEG which provided a more accurate and robust classification scheme with *F1* score well above 90% for the automatic Spike detection.

In conclusion, we successfully built a robust Spike detection scheme comprising a feature extraction and a classification

step. These preliminary results could form the basis for establishing EMEG as a powerful tool for non-invasive presurgical epilepsy diagnosis.

REFERENCES

[1] "World health organization," https://www.who.int, 2021.

[2] M.-C. Picot, A. Jaussent, D. Neveu, P. Kahane, A. Crespel, P. Gelisse, E. Hirsch, P. Derambure, S. Dupont, E. Landré *et al.*, "Cost-effectiveness analysis of epilepsy surgery in a controlled cohort of adult patients with intractable partial epilepsy: a 5-year follow-up study," *Epilepsia*, vol. 57, no. 10, pp. 1669–1679, 2016.

[3] S. West, S. J. Nolan, and R. Newton, "Surgery for epilepsy: a systematic review of current evidence," *Epileptic Disorders*, vol. 18, no. 2, pp. 113–121, 2016.

[4] H. O. Lüders, I. Najm, D. Nair, P. Widdess-Walsh, and W. Bingman, "The epileptogenic zone: general principles," *Epileptic disorders*, vol. 8, no. 2, pp. 1–9, 2006.

[5] Z. Fitzgerald, M. Morita-Sherman, O. Hogue, B. Joseph, M. K. Alvim, C. L. Yasuda, D. Vegh, D. Nair, R. Burgess, W. Bingaman *et al.*, "Improving the prediction of epilepsy surgery outcomes using basic scalp eeg findings," *Epilepsia*.

[6] G. Dassios, A. S. Fokas, and D. Hadjiloizi, "On the complementarity of electroencephalography and magnetoencephalography," *Inverse Problems*, vol. 23, no. 6, p. 2541, 2007.

[7] M.-X. Huang, T. Song, D. J. Hagler Jr, I. Podgorny, V. Jousmaki, L. Cui, K. Gaa, D. L. Harrington, A. M. Dale, R. R. Lee *et al.*, "A novel integrated meg and eeg analysis method for dipolar sources," *Neuroimage*, vol. 37, no. 3, pp. 731–748, 2007.

[8] Ü. Aydin, S. Rampp, A. Wollbrink, H. Kugel, J.-H. Cho, T. R. Knösche, C. Grova, J. Wellmer, and C. Wolters, "Zoomed mri guided by combined eeg/meg source analysis: a multimodal approach for optimizing presurgical epilepsy work-up and its application in a multi-focal epilepsy patient case study," *Brain topography*, vol. 30, no. 4, pp. 417–433, 2017.

[9] Ü. Aydin, J. Vorwerk, M. Dümpelmann, P. Küpper, H. Kugel, M. Heers, J. Wellmer, C. Kellinghaus, J. Haueisen, S. Rampp *et al.*, "Combined eeg/meg can outperform single modality eeg or meg source reconstruction in presurgical epilepsy diagnosis," *PloS one*, vol. 10, no. 3, p. e0118753, 2015.

[10] M. Iwasaki, E. Pestana, R. C. Burgess, H. O. Lüders, H. Shamoto, and N. Nakasato, "Detection of epileptiform activity by human interpreters: blinded comparison between electroencephalography and magnetoencephalography," *Epilepsia*, vol. 46, no. 1, pp. 59–68, 2005.

[11] S. Knake, E. Halgren, H. Shiraishi, K. Hara, H. Hamer, P. Grant, V. Carr, D. Foxe, S. Camposano, E. Busa *et al.*, "The value of multichannel meg and eeg in the presurgical evaluation of 70 epilepsy patients," *Epilepsy research*, vol. 69, no. 1, pp. 80–86, 2006.

[12] J. S. Ebersole and M. Wagner, "Relative yield of meg and eeg spikes in simultaneous recordings," *Journal of Clinical Neurophysiology*, vol. 35, no. 6, pp. 443–453, 2018.

[13] A. R. Johansen, J. Jin, T. Maszczyk, J. Dauwels, S. S. Cash, and M. B. Westover, "Epileptiform spike detection via convolutional neural networks," in *2016 IEEE International Conference on Acoustics, Speech and Signal Processing (ICASSP)*. IEEE, 2016, pp. 754–758.

[14] F. E. Abd El-Samie, T. N. Alotaiby, M. I. Khalid, S. A. Alshebeili, and S. A. Aldosari, "A review of eeg and meg epileptic spike detection algorithms," *IEEE Access*, vol. 6, pp. 60 673–60 688, 2018.

[15] W. Webber, B. Litt, K. Wilson, and R. Lesser, "Practical detection of epileptiform discharges (eds) in the eeg using an artificial neural network: a comparison of raw and parameterized eeg data," *Electroencephalography and clinical Neurophysiology*, vol. 91, no. 3, pp. 194–204, 1994.

[16] A. J. Gabor and M. Seyal, "Automated interictal eeg spike detection using artificial neural networks," *Electroencephalography and clinical Neurophysiology*, vol. 83, no. 5, pp. 271–280, 1992.

[17] M. I. Khalid, T. Alotaiby, S. A. Aldosari, S. A. Alshebeili, M. H. Al-Hameed, F. S. Y. Almohammed, and T. S. Alotaibi, "Epileptic meg spikes detection using common spatial patterns and linear discriminant analysis," *IEEE Access*, vol. 4, pp. 4629–4634, 2016.

[18] Z. H. Inan and M. Kuntalp, "A study on fuzzy c-means clustering-based systems in automatic spike detection," *Computers in biology and medicine*, vol. 37, no. 8, pp. 1160–1166, 2007.

[19] M. Feucht, K. Hoffmann, K. Steinberger, H. Witte, F. Benninger, M. Arnold, and A. Doering, "Simultaneous spike detection and topographic classification in pediatric surface eegs," *NeuroReport*, vol. 8, no. 9, pp. 2193–2197, 1997.

[20] M. C. Tjepkema-Cloostermans, R. C. de Carvalho, and M. J. van Putten, "Deep learning for detection of focal epileptiform discharges from scalp eeg recordings," *Clinical neurophysiology*, vol. 129, no. 10, pp. 2191–2196, 2018.

[21] C. da Silva Lourenço, M. C. Tjepkema-Cloostermans, and M. J. van Putten, "Efficient use of clinical eeg data for deep learning in epilepsy," *Clinical Neurophysiology*, vol. 132, no. 6, pp. 1234–1240, 2021.

[22] M. Antonakakis, S. Rampp, C. Kellinghaus, C. H. Wolters, and G. Moeddel, "Individualized targeting and optimization of multi-channel transcranial direct current stimulation in drug-resistant epilepsy," in *2019 IEEE 19th International Conference on Bioinformatics and Bioengineering (BIBE)*. IEEE, 2019, pp. 871–876.

[23] J. M. Palva, S. H. Wang, S. Palva, A. Zhigalov, S. Monto, M. J. Brookes, J.-M. Schoffelen, and K. Jerbi, "Ghost interactions in meg/eeg source space: A note of caution on inter-areal coupling measures," *Neuroimage*, vol. 173, pp. 632–643, 2018.

[24] L. R. Quitadamo, R. Mai, F. Gozzo, V. Pelliccia, F. Cardinale, and S. Seri, "Kurtosis-based detection of intracranial high-frequency oscillations for the identification of the seizure onset zone," *International journal of neural systems*, vol. 28, no. 07, p. 1850001, 2018.

[25] K. M. Tsiouris, V. C. Pezoulas, M. Zervakis, S. Konitsiotis, D. D. Koutsouris, and D. I. Fotiadis, "A long short-term memory deep learning network for the prediction of epileptic seizures using eeg signals," *Computers in biology and medicine*, vol. 99, pp. 24–37, 2018.

[26] N. Kannathal, M. L. Choo, U. R. Acharya, and P. Sadasivan, "Entropies for detection of epilepsy in eeg," *Computer methods and programs in biomedicine*, vol. 80, no. 3, pp. 187–194, 2005.

[27] M. De Curtis and G. Avanzini, "Interictal spikes in focal epileptogenesis," *Progress in neurobiology*, vol. 63, no. 5, pp. 541–567, 2001.

[28] M. Antonakakis, S. I. Dimitriadis, M. Zervakis, A. C. Papanicolaou, and G. Zouridakis, "Aberrant whole-brain transitions and dynamics of spontaneous network microstates in mild traumatic brain injury," *Frontiers in computational neuroscience*, vol. 13, p. 90, 2020.

[29] M. Antonakakis, S. I. Dimitriadis, M. Zervakis, S. Micheloyannis, R. Rezaie, A. Babajani-Feremi, G. Zouridakis, and A. C. Papanicolaou, "Altered cross-frequency coupling in resting-state meg after mild traumatic brain injury," *International Journal of Psychophysiology*, vol. 102, pp. 1–11, 2016.

[30] E. Bullmore and O. Sporns, "Complex brain networks: graph theoretical analysis of structural and functional systems," *Nature reviews neuroscience*, vol. 10, no. 3, pp. 186–198, 2009.

[31] S. I. Dimitriadis, G. Zouridakis, R. Rezaie, A. Babajani-Feremi, and A. C. Papanicolaou, "Functional connectivity changes detected with magnetoencephalography after mild traumatic brain injury," *NeuroImage: Clinical*, vol. 9, pp. 519–531, 2015.

[32] M. Rubinov and O. Sporns, "Complex network measures of brain connectivity: uses and interpretations," *Neuroimage*, vol. 52, no. 3, pp. 1059–1069, 2010.

[33] R. Garreta and G. Moncecchi, *Learning scikit-learn: machine learning in python*. Packt Publishing Ltd, 2013.

[34] S. B. Wilson, C. A. Turner, R. G. Emerson, and M. L. Scheuer, "Spike detection ii: automatic, perception-based detection and clustering," *Clinical neurophysiology*, vol. 110, no. 3, pp. 404–411, 1999.

[35] P. Valenti, E. Cazamajou, M. Scarpettini, A. Aizemberg, W. Silva, and S. Kochen, "Automatic detection of interictal spikes using data mining models," *Journal of neuroscience methods*, vol. 150, no. 1, pp. 105–110, 2006.

[36] T. P. Exarchos, C. Papaloukas, D. I. Fotiadis, and L. K. Michalis, "An association rule mining-based methodology for automated detection of ischemic ecg beats," *IEEE transactions on biomedical engineering*, vol. 53, no. 8, pp. 1531–1540, 2006.

[37] A. Ossadtchi, S. Baillet, J. Mosher, D. Thyerlei, W. Sutherling, and R. Leahy, "Automated interictal spike detection and source localization in magnetoencephalography using independent components analysis and spatio-temporal clustering," *Clinical Neurophysiology*, vol. 115, no. 3, pp. 508–522, 2004.